PRELIMINARY STUDIES ON SODIUM ALGINATE AND POLY(VINYL ALCOHOL) HYDROGELS MODIFIED WITH INSULIN-LOADED CHITOSAN MICROSPHERES FOR DIABETIC WOUND TREATMENT

Agnieszka Kłapcia [1]*, Patrycja Domalik-Pyzik [2]

[1] AGH University of Krakow, Academic Centre for Materials and Nanotechnology, 30-059 Krakow, Poland
[2] AGH University of Krakow, Faculty of Materials Science and Ceramics, Department of Biomaterials and Composites, al. A. Mickiewicza 30, 30-059 Krakow, Poland

* E-mail: aklapcia@agh.edu.pl

Abstract

Diabetic wounds, a common complication of diabetes, often lead to chronic ulcerations and infections on the lower limbs. Conventional treatments are expensive and often inadequate for advanced cases, necessitating the development of innovative approaches, such as hydrogel-based dressings that support tissue reconstruction and enable the delivery of biologically active substances. This study aimed to develop a multifunctional hydrogel dressing for insulin delivery in diabetic wounds. A hydrogel matrix composed of sodium alginate and poly(vinyl alcohol), modified with allantoin, was created. Insulin-loaded chitosan microspheres were incorporated to enhance the effects of growth factors and regulate glucose levels around the wound site. The research focused on preparing the hydrogel matrix, cross-linking, encapsulating insulin in chitosan microspheres, and evaluating material properties. We assessed microstructure, chemical stability, water absorption, and insulin release kinetics. Fourier-transform infrared spectroscopy (FTIR) and elemental analysis confirmed the presence of insulin and allantoin in the matrix. Hydrated microspheres had diameters ranging from 1089 to 1549 μm, while dehydrated microspheres ranged from 471 to 622 μm. Absorbency was approximately 500% for unbuffered and 1000-1500% for buffered microspheres. Rheological tests confirmed cross-linking of the Alg-PVA sol via cyclic freezing-thawing and specific solutions. Chemical stability tests showed about 40% mass degradation of the Alg-PVA hydrogel over 4 weeks. Overall, the results indicate that the developed hydrogel composition holds potential for further research and development.

Keywords: *diabetic wounds, insulin, sodium alginate, poly(vinyl alcohol), multifunctional hydrogel systems, drug delivery systems*

[Engineering of Biomaterials 174 (2026) 04]

doi:10.34821/eng.biomat.174.2026.04

Submitted: 2025-12-28, Accepted: 2026-02-23, Published: 2026-02-28

Copyright © 2026 by the authors. Some rights reserved.
Except otherwise noted, this work is licensed under
https://creativecommons.org/licenses/by/4.0

Introduction

Diabetic wounds, particularly diabetic foot ulcers, are a severe complication of diabetes and a leading cause of hospitalization and limb amputation worldwide [1]. These wounds are difficult to heal due to persistent hyperglycaemia, impaired immunity, chronic inflammation, and frequent infections [2], [3]. The likelihood of a patient developing a diabetic foot ulcer (DFU) increases with the duration of their diabetes, with patients with established diabetic wounds having a significant risk of amputation (17% of patients with a new DFU require a minor amputation and 5% of patients need a major amputation within a year of diagnosis) [4]. In turn, the estimated five-year risk of death is 2.5 times higher in people with DFU than in people with diabetes alone, and the five-year mortality rate for diabetes-related amputations exceeds 70%, which is worse than for many common cancers [5]

The main reason for the difficulty in treating these wounds is the persistent hyperglycemia, which weakens the overall immunity of patients and also contributes to the prolonged duration of inflammation in the wounds and the prolonged wound healing process [3]. The wound healing process in diabetes is disrupted at multiple stages, with prolonged inflammation, excessive production of reactive oxygen species (ROS), and accumulation of advanced glycation end-products (AGEs) contributing to poor tissue regeneration and increased susceptibility to infection [6], [7], [8], [9], [10]. As a result, diabetic wounds often exhibit delayed angiogenesis, reduced collagen content, and impaired mechanical strength, leading to frequent recurrence and chronicity [7], [11].

Conventional wound dressings such as gauze and bandages provide basic protection but do not adequately support the complex healing needs of diabetic wounds [12]. In contrast, hydrogel-based dressings offer a moist environment, promote tissue regeneration, and can be engineered to deliver bioactive substances[13], [14].

Recent advances have focused on multifunctional hydrogels with antimicrobial, anti-inflammatory, and drug delivery capabilities to address the multifactorial challenges of diabetic wound healing [15], [16].

Insulin, beyond its metabolic role, has demonstrated anti-inflammatory and regenerative effects in wound healing. However, local delivery is challenging due to rapid degradation and the need for controlled release. In order to overcome the barriers to insulin delivery to the body, a number of drug delivery systems (DDSs) have been developed to control the pharmacokinetic profile of its different analogues. Hydrogel systems incorporating micro – and nanocarriers for insulin delivery represent a promising strategy for improving diabetic wound outcomes. The therapeutic efficacy of such solutions depends on many factors related to pharmacokinetics, distribution, cellular uptake, metabolism, excretion, and toxicity, which depend on the method and route of administration [17], [18], [19], [20], [21].

This study presents the development and characterization of a multifunctional hydrogel dressing composed of sodium alginate and poly(vinyl alcohol), incorporating chitosan microspheres loaded with insulin and allantoin, as a potential solution for enhanced diabetic wound care. TABLE 1 summarizes the list of sample names and the concentrations of the corresponding materials.

TABLE 1. Sample names and concentrations of the corresponding materials.

Sample Name	Description
Cs + Lac	Empty chitosan microspheres obtained from a 1.5% aqueous chitosan solution and 1% lactic acid.
Cs + Lac + Alan	Chitosan microspheres obtained from a 1.5% aqueous chitosan solution and 1% lactic acid, loaded with allantoin at 5% relative to the dry weight of the chitosan polymer.
Cs + Lac + Alan + Ins	Chitosan empty microspheres obtained from a 1.5% aqueous chitosan solution and 1% lactic acid, loaded with allantoin at 5% relative to the dry weight of the chitosan polymer, containing approximately 100 units of insulin per production batch.
Cs + Ac	Empty chitosan microspheres obtained from a 1.5% aqueous chitosan solution and 1% acetic acid.
Cs + Ac + Alan	Chitosan microspheres obtained from a 1.5% aqueous chitosan solution and 1% acetic acid, loaded with allantoin at 5% relative to the dry weight of the chitosan polymer.
Cs + Lac + Alan + Ins	Chitosan empty microspheres obtained from a 1.5% aqueous chitosan solution and 1% acetic acid, loaded with allantoin at 5% relative to the dry weight of the chitosan polymer, containing approximately 100 units of insulin per production batch.
Alg-PVA	A hydrogel based on alginate and PVA in a 7:3 mass ratio, crosslinked with 1.0/1.5% $ZnSO_4$. In the samples containing microspheres, 2 wt% (relative to the dry weight of the polymer powders used to produce the hydrogels) of various types of obtained microspheres was incorporated.

Materials and Methods

Materials

The following reagents were used in this work: sodium alginate (Alg, Mw 450,000-550,000, Thermo-Scientific) and poly(vinyl alcohol) (PVA, Mowiol 20-98, Mw ~125,000, Sigma-Aldrich) were used to prepare the polymer matrix; sodium dihydrogen phosphate (V) Na_2HPO_4 (POCH, Poland), zinc sulfate (VI) $ZnSO_4$ (POCH, Poland), and calcium chloride $CaCl_2$ (Sigma-Aldrich) were used in the cross-linking process. Medium molecular weight chitosan (Cs), lactic acid (Lac, 88% CZDA, POCH, Poland), acetic acid (Ac, 99.5%-99.9% CZDA, POCH, Poland), sodium tripolyphosphate (TPP, Acros-Organics), sodium chloride (NaCl, POCH, Poland), and Span80 (Sigma-Aldrich) were used in the process of obtaining microspheres. Allantoin (Alan, Sigma-Aldrich) and insulin (Ins) – Liprolog KwikPen and Gensulin R were selected as active biological substances intended for encapsulation.

Preparation of chitosan microspheres

Chitosan microspheres were prepared by dissolving chitosan powder (1.5% w/v) in either 1% lactic acid or 1% acetic acid, followed by magnetic stirring at 250 rpm for 20 hours. The resulting solutions were labeled Cs+Lac and Cs+Ac, respectively. For allantoin-modified microspheres, an aqueous allantoin solution (4 mg/ml) was added to achieve a final concentration of 5% (w/w) relative to the dry chitosan. The chitosan solutions (with or without allantoin) were added dropwise through a 0.7 mm straight-ended needle into a continuously stirred cross-linking bath containing 5% tripolyphosphate (TPP), 0.25 mol/dm³ sodium chloride (NaCl), and 2% Span80, at a solution-to-bath volume ratio of 1:10. Microspheres were left in the cross-linking bath for at least 48 hours to ensure complete cross-linking, then collected, drained, and washed sequentially with isopropanol, 70% ethanol, and distilled water. The final microspheres were either dried or stored refrigerated for further use. For insulin-loaded microspheres, the Cs+Lac solution was buffered to pH 6 using 0.1 mol/dm³ sodium hydroxide (NaOH) before cross-linking, to protect insulin from degradation. These microspheres were cross-linked at room temperature for 2 hours and then stored in a refrigerator until cross-linking was complete. Two insulin formulations, Lispro (200 IU/mL) and Gensulin R (100 IU/mL), were used, with 100 units of insulin encapsulated per 2.5 mL of Cs+Lac solution. Allantoin – and insulin-modified microspheres were prepared using the same procedure. The preparation scheme is illustrated in FIG. 1.

Preparation of the hydrogel matrix

Hydrogel matrices were prepared by blending sodium alginate and poly(vinyl alcohol) (PVA) in mass ratios of 3:7 or 7:3. Pre-weighed polymers were dissolved in 0.4% NaH_2PO_4 solution under magnetic stirring and heating (up to 90°C) to achieve a final polymer concentration of 2% (w/v). The resulting homogeneous solutions (approximately 30 g each) were cast into Petri dishes and subjected to three freeze–thaw cycles (24 hours at –20°C, followed by 6 hours at room temperature) for initial cross-linking. For modified hydrogels, Cs+Lac+Alan or Cs+Ac+Alan microspheres were incorporated at 2% (w/w, relative to dry polymer mass) before cross-linking. Since freeze–thaw cycling primarily stabilizes PVA, an additional cross-linking step was performed for 7Alg-3PVA samples using either 1% $CaCl_2$ or 1% $ZnSO_4$ aqueous solutions.

Phase separation occurred in samples cross-linked with $CaCl_2$, while $ZnSO_4$-cross-linked samples formed uniform hydrogels without phase separation. For Alg-PVA hydrogels cross-linked with 1% $ZnSO_4$, gelation began immediately upon mixing, with full stabilization within 6–8 minutes and increased viscosity after 24 hours. Based on these results, $ZnSO_4$ was selected as the cross-linking agent for further studies.

Preparation of multifunctional hydrogel systems

In the final stage, the target materials were prepared (FIG. 2). Based on the tests conducted, the 7Alg-3PVA system was selected as the matrix material, employing a combined cross-linking method. Approximately 1.5 mL of solutions of both polymers, either modified or unmodified with allantoin (5% w/w), were placed in the wells of a 24-well plate.

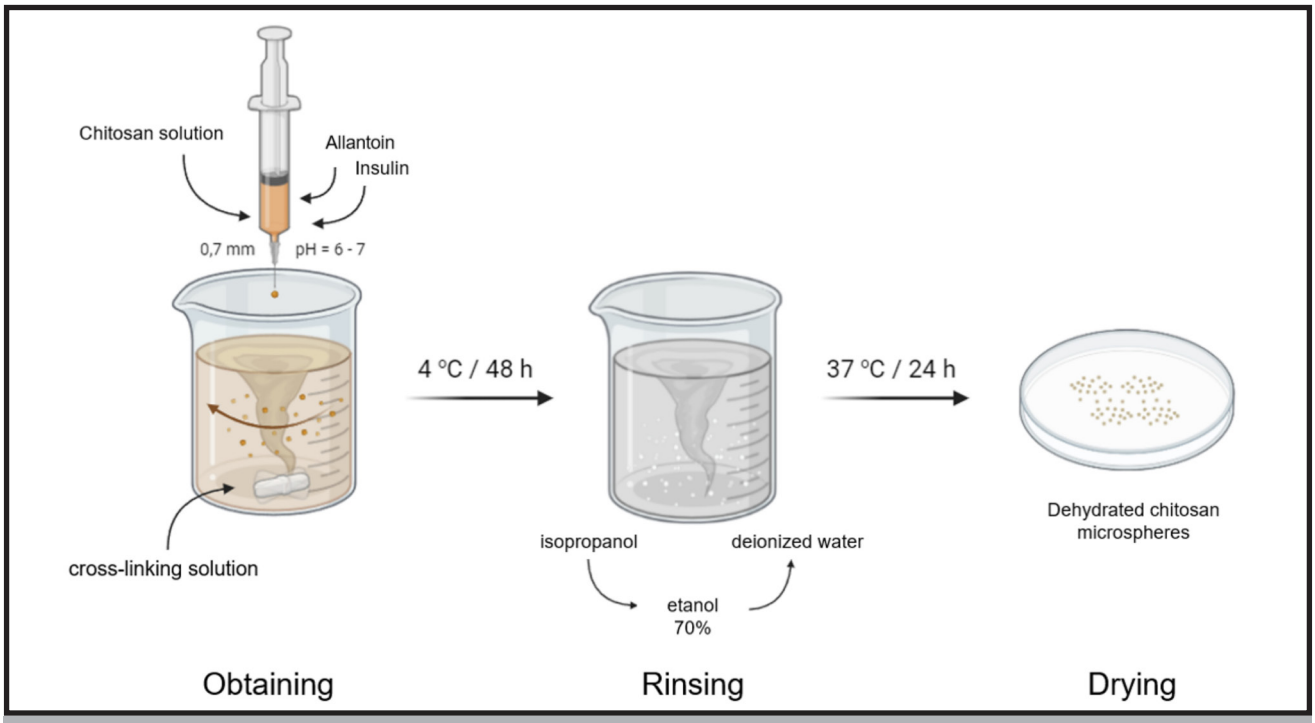

FIG. 1. Schematic illustration of the preparation of chitosan microspheres loaded with insulin and allantoin via cross-linking emulsification.

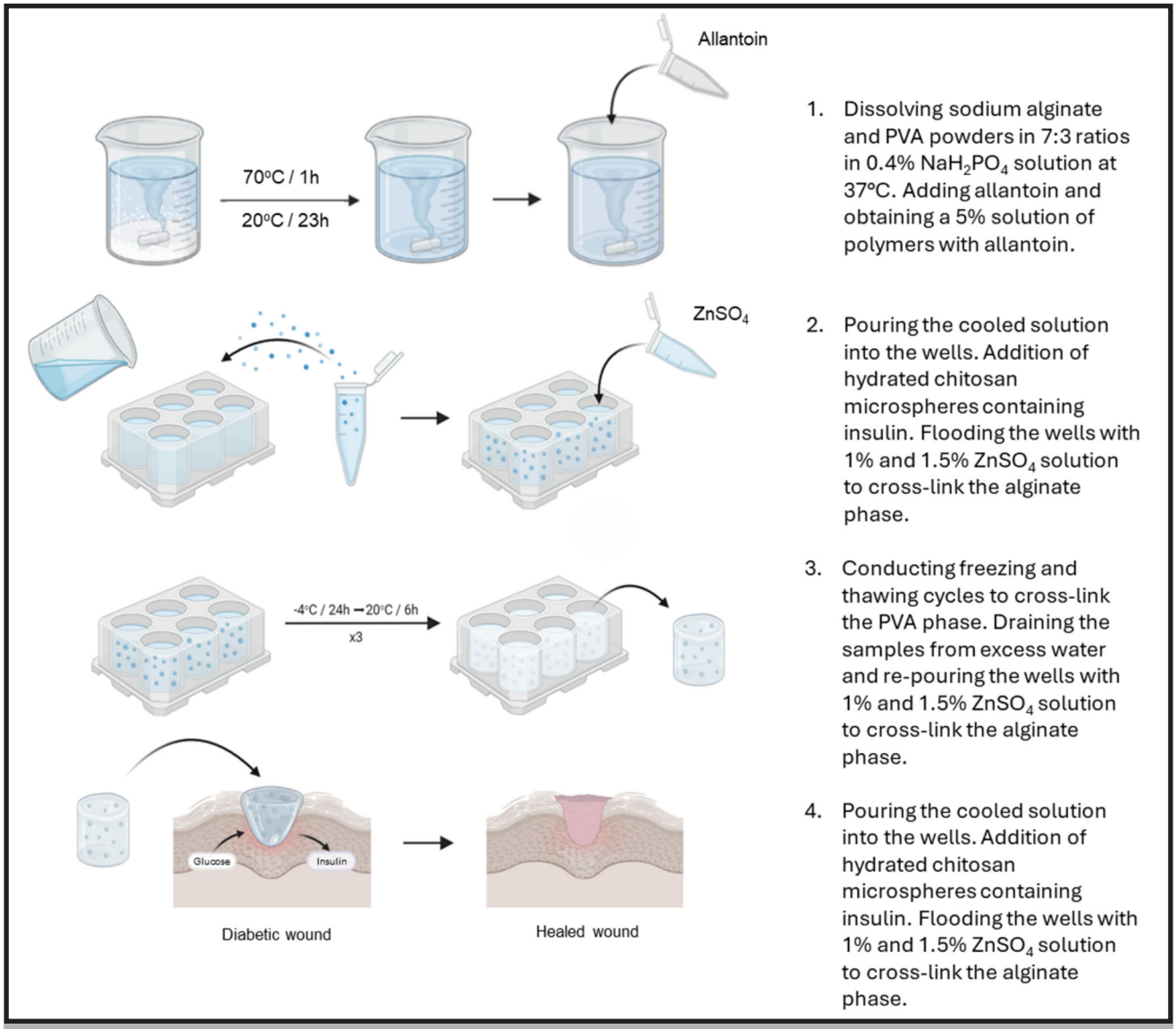

FIG. 2. Schematic illustration of the fabrication of Alg–PVA hydrogels incorporating allantoin and insulin-loaded chitosan microspheres.

Approximately 30 Cs+Lac microspheres were also added to some of the wells. The samples underwent cross-linking using 1% and 1.5% $ZnSO_4$ solutions in a 1:1 volume ratio with the polymer solution. Subsequently, they were subjected to cyclic freezing and thawing. After the completion of the third cycle, excess water was drained from the wells, and the samples were refilled with 1% and 1.5% $ZnSO_4$ solution. Samples intended for microscopic examination were frozen at −20°C and lyophilized for 48 hours using a Labconco Freezone.

Characterization methods

Optical Microscopy

Hydrated and dried microspheres (buffered and unbuffered) were imaged using a Keyence VHX 900F digital optical microscope at 20×, 50×, 100×, and 150× magnifications. Diameters of 20 microspheres per group were measured using ImageJ, followed by statistical analysis.

Scanning Electron Microscopy (SEM)

Samples were mounted on holders with carbon adhesive tape and coated with a 10 nm carbon layer by sputtering. SEM imaging was performed using an Apreo 2S (Thermo Scientific) equipped with EDAX for elemental analysis.

Structural Analysis (FTIR ATR)

Fourier Transform Infrared Spectroscopy with Attenuated Total Reflectance (FTIR ATR) was performed using a Bruker FTIR Tensor 27 spectrometer (Opus software). Spectra were recorded at 4 cm^{-1} resolution, 4000–400 cm^{-1} range, with 64 scans per sample. Data were processed using SpectraGryph.

Microsphere Water Absorption Test

Wet microspheres from each experimental group (unbuffered and buffered) were filtered using filter paper and weighed on an analytical balance. Samples were then dried at 37°C for 24 hours until constant mass and reweighed. Water absorption (%) was calculated as (wet mass – dry mass) / dry mass × 100. For each group, the mean and standard deviation were determined from three independent measurements. Measurement uncertainty was estimated using Gauss's law of propagation, with a balance resolution of 0.001 g.

Rheological Properties

Hydrogel rheology was assessed using an Anton Paar MCR 302 rheometer (RheoCompass software) in a plate-plate system (gap: 1 mm, max pressure: 0.07 N) at 37°C. Storage and loss moduli were measured over 5 minutes (30 intervals). Shear stress-strain and frequency sweeps (100–0.1 rad/s, 15 min) were performed. Cross-linking efficiency was evaluated for 2% Alg-PVA hydrogels with $ZnSO_4$ concentrations from 0-3.0%. The effect of allantoin and $ZnSO_4$ concentration (1% vs. 1.5%) on hydrogel discs was also compared.

Chemical Stability

Hydrogel discs cross-linked with 1% or 1.5% $ZnSO_4$ were immersed in Ringer's solution (sample:solution ratio 1:20) and incubated at 37°C for 4 weeks. Samples were weighed after 7, 14, 21, and 28 days to determine mass loss (%). Measurement uncertainty was calculated using Gauss's law, with a balance accuracy of 0.001 g.

Results and Discussions

Morphology and microstructure

Hydrated microspheres exhibited diameters ranging from 1089 to 1549 µm, while dried microspheres ranged from 471 to 622 µm, corresponding to approximately 50% volumetric shrinkage upon drying (FIG.3). Unbuffered microspheres displayed a more regular, spherical shape with smooth surfaces, whereas buffered microspheres were less spherical and exhibited irregular, layered surfaces. These differences are attributed to variations in pH and cross-linking conditions during synthesis. Incorporation of allantoin and insulin did not significantly alter the overall size distribution but did affect surface texture and water absorption capacity.

SEM analysis (FIG. 4) revealed that chitosan microspheres possessed a highly developed surface topology with numerous pits, depressions, and irregularities, which may facilitate further functionalization or drug loading.

Optical microscopy (FIG. 5) demonstrated that hydrogels without allantoin were more transparent, while allantoin-modified hydrogels appeared slightly opaque and contained visible water bubbles and PVA precipitates. The internal structure of the hydrogels was heterogeneous, with a stratified arrangement: the outer regions were more transparent (PVA-rich), and the central region was more opaque (alginate-rich), suggesting partial phase separation during cross-linking. SEM imaging of lyophilized

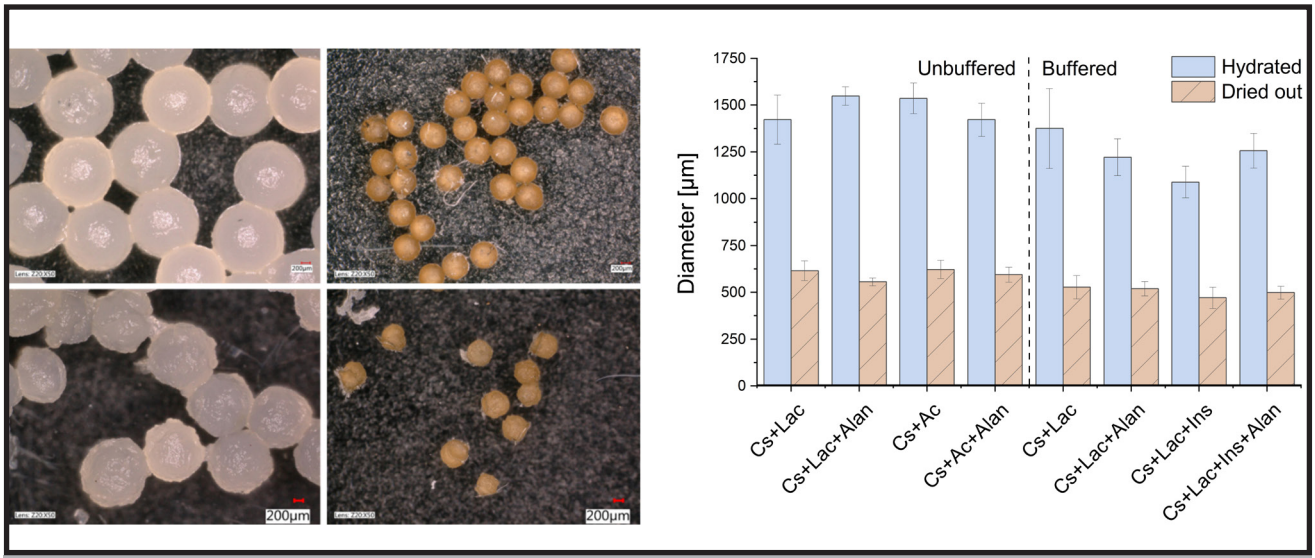

FIG. 3. (Left) Optical microscopy images of Cs+Lac+Alan microspheres at 50× magnification: upper left—unbuffered, hydrated; upper right—unbuffered, dried; lower left—buffered, hydrated; lower right—buffered, dried. (Right) Average diameters of wet and dry unbuffered and buffered microspheres.

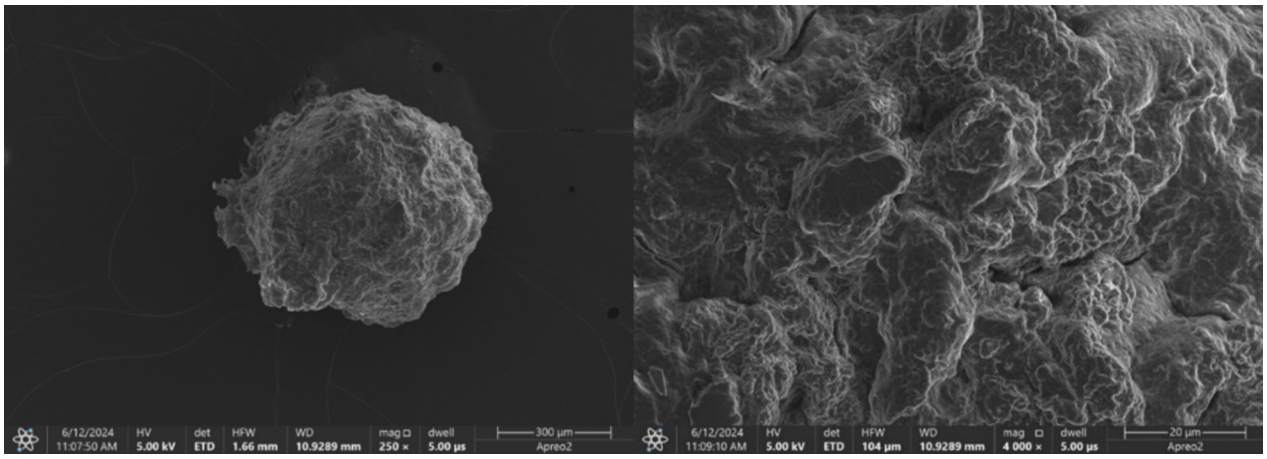

FIG. 4. SEM image of chitosan microsphere at 250× (left) and at 4000× (right) magnification.

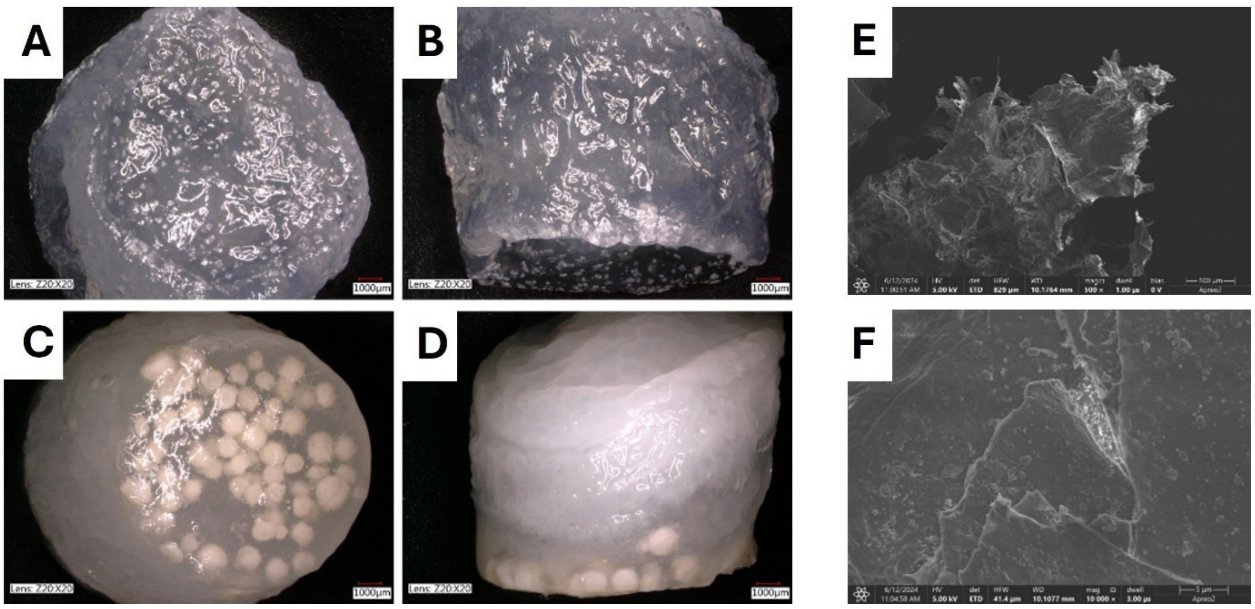

FIG. 5. Optical microscopy images (20× magnification; scale bar: 1000 µm) of Alg–PVA hydrogels prepared using 1.5% $ZnSO_4$ and 5% allantoin solution: bottom (A) and side (B) views; and Alg–PVA hydrogels containing CS microspheres: bottom (C) and side (D) views. SEM images of freeze-dried Alg–PVA hydrogels at 500× (E) and 10,000× (F) magnification.

hydrogels cross-linked with 1.5% $ZnSO_4$ revealed a low-porosity, plate-like network structure typical of alginate-PVA hydrogels. The observed morphology is consistent with previously reported structures for similar hydrogel systems [22].

The morphological analysis indicates that both the fabrication method and cross-linking conditions significantly influence microsphere shape, surface characteristics, and hydrogel internal architecture. While the microspheres offer a high surface area for potential drug delivery, the hydrogel matrices exhibit a heterogeneous, low-porosity structure, which may impact cell infiltration and tissue integration.

Water absorption test

The test was performed on samples of unbuffered microspheres obtained using lactic and acetic acids, and buffered microspheres obtained using lactic acid and containing insulin. FIG. 6 presents a comparison of the water absorption of unbuffered and buffered microspheres obtained using lactic and acetic acids.

Based on the results, it was found that unbuffered microsphere samples were generally characterized by lower water absorption compared to buffered samples. Comparing unbuffered samples of the Cs+Lac and Cs+Lac+Alan types with buffered counterparts, it was shown that the water absorption of buffered samples is 1.9 times higher for Cs+Lac samples and over 2.8 times higher for Cs+Lac+Alan samples. This is most likely due to the influence of higher pH in the process of obtaining microspheres, as well as the longer time the microspheres were left in the cross-linking solution and the longer drying process of buffered microspheres than in the case of unbuffered microspheres. The unbuffered samples were characterized by an average 4.6-fold reduction in their mass after water removal, with the lowest water absorption for sample Cs+Lac and the highest for sample Cs+Lac+Alan. In turn, the buffered samples were characterized by an average 12-fold reduction in their mass after water removal, with the lowest water absorption for sample Cs+Lac and the highest for sample Cs+Lac+Ins.

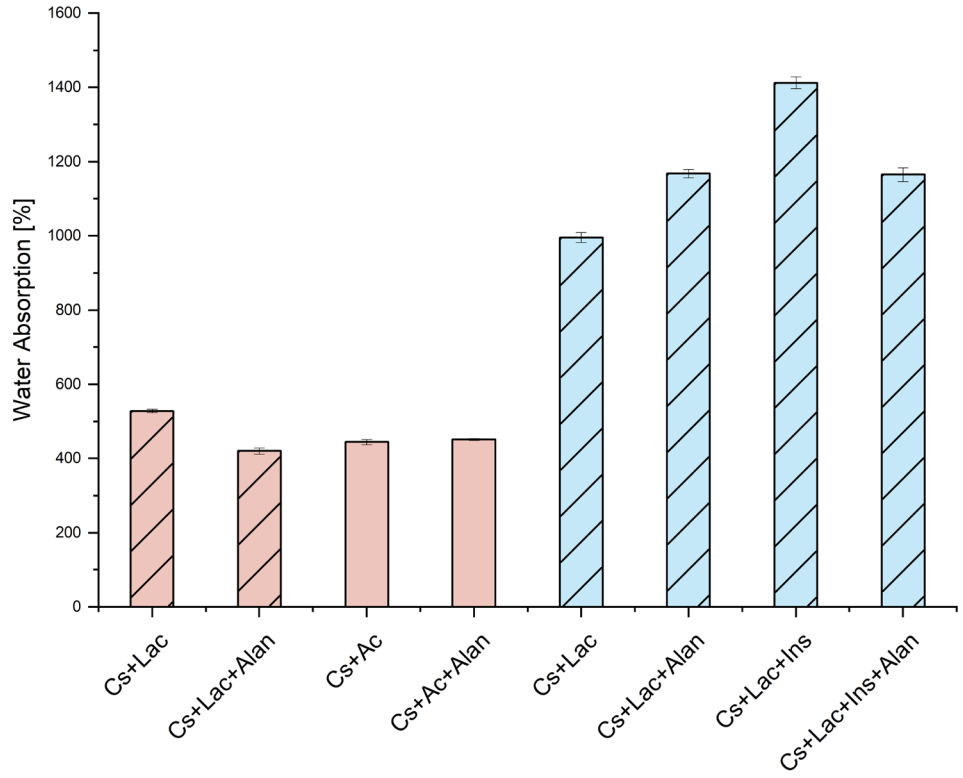

FIG. 6. Water absorption of unbuffered microspheres (salmon-colored bars) and buffered microspheres (light blue bars). Microspheres prepared using lactic acid are indicated by diagonal shading.

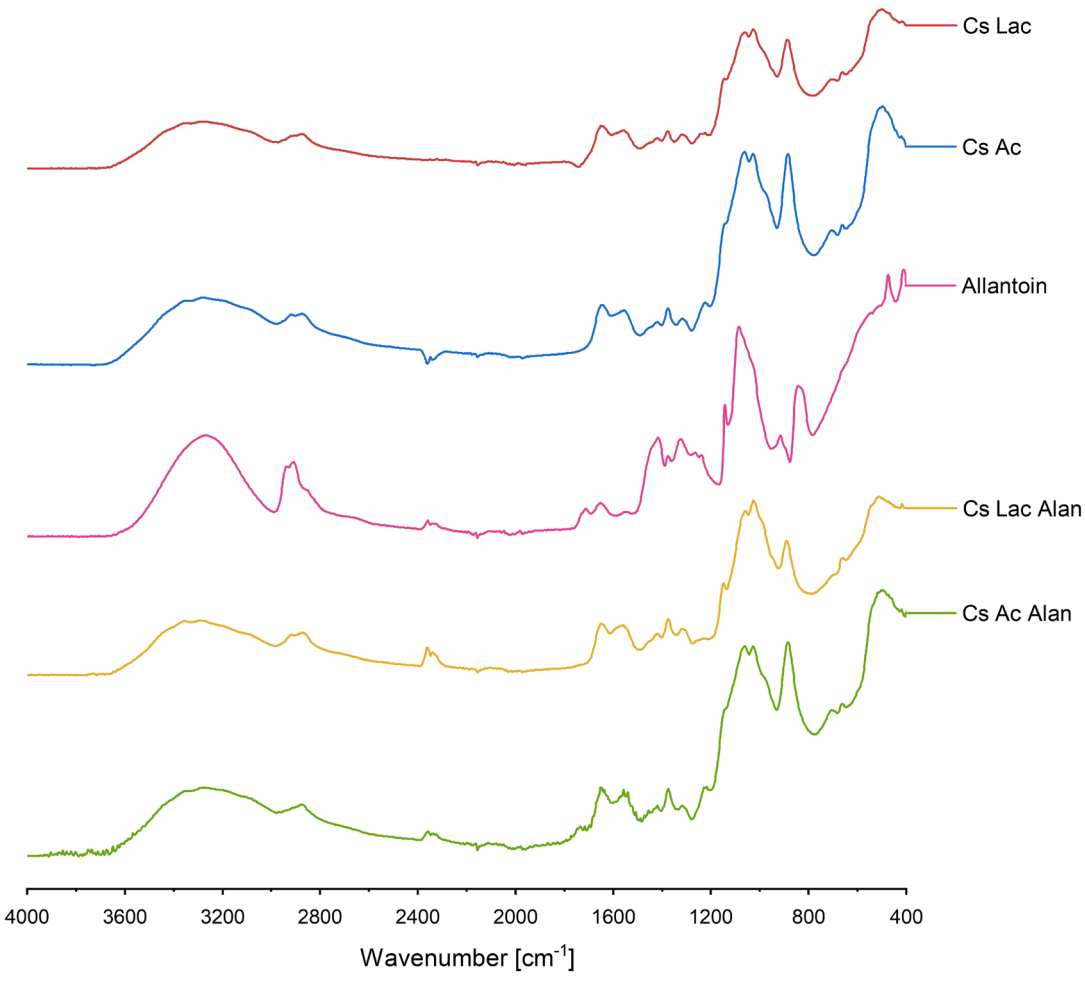

FIG. 7. FTIR spectra of samples: Cs+Lac, Cs+Lac+Alan, allantoin, Cs+Ac, and Cs+Ac+Alan.

Chemical structure and composition: FTIR and EDS analysis

FTIR and EDS were used to confirm the successful incorporation of allantoin and insulin into chitosan microspheres and the hydrogel matrix, and to analyze the chemical interactions between the components. FTIR-ATR spectra were obtained for chitosan microspheres prepared with lactic acid (Cs+Lac), with and without allantoin (Cs+Lac+Alan), insulin (Cs+Lac+Ins), and both (Cs+Lac+Ins+Alan), as well as for reference allantoin and acetic acid-based samples (FIGs 7 and 8, TABLE 2). In allantoin-modified samples, a shift and increased intensity at 2918 cm^{-1} (from 2915 cm^{-1} in unmodified) and a reduction at 2873 cm^{-1} were observed, suggesting altered N-H bond interactions within the chitosan structure. The 1558 cm^{-1} band (N-H bending) was more pronounced in allantoin-modified samples, while reduced intensities at 1147, 1058, and 891 cm^{-1} indicated interactions between allantoin and chitosan, particularly in C-O and C-H bond regions. Insulin-loaded microspheres exhibited stronger absorbance at ~2920 cm^{-1} and a split of the 2875 cm^{-1} band into two peaks at lower wavenumbers, indicating N-H group interactions. In the amide I (1650 cm^{-1}) and amide II (1560 cm^{-1}) regions, insulin-loaded samples showed higher intensity and a shift toward higher wavenumbers (from 1648 cm^{-1} to 1642 cm^{-1}), consistent with peptide bond contributions. The C-H stretching region (~890 cm^{-1}) showed reduced intensity,

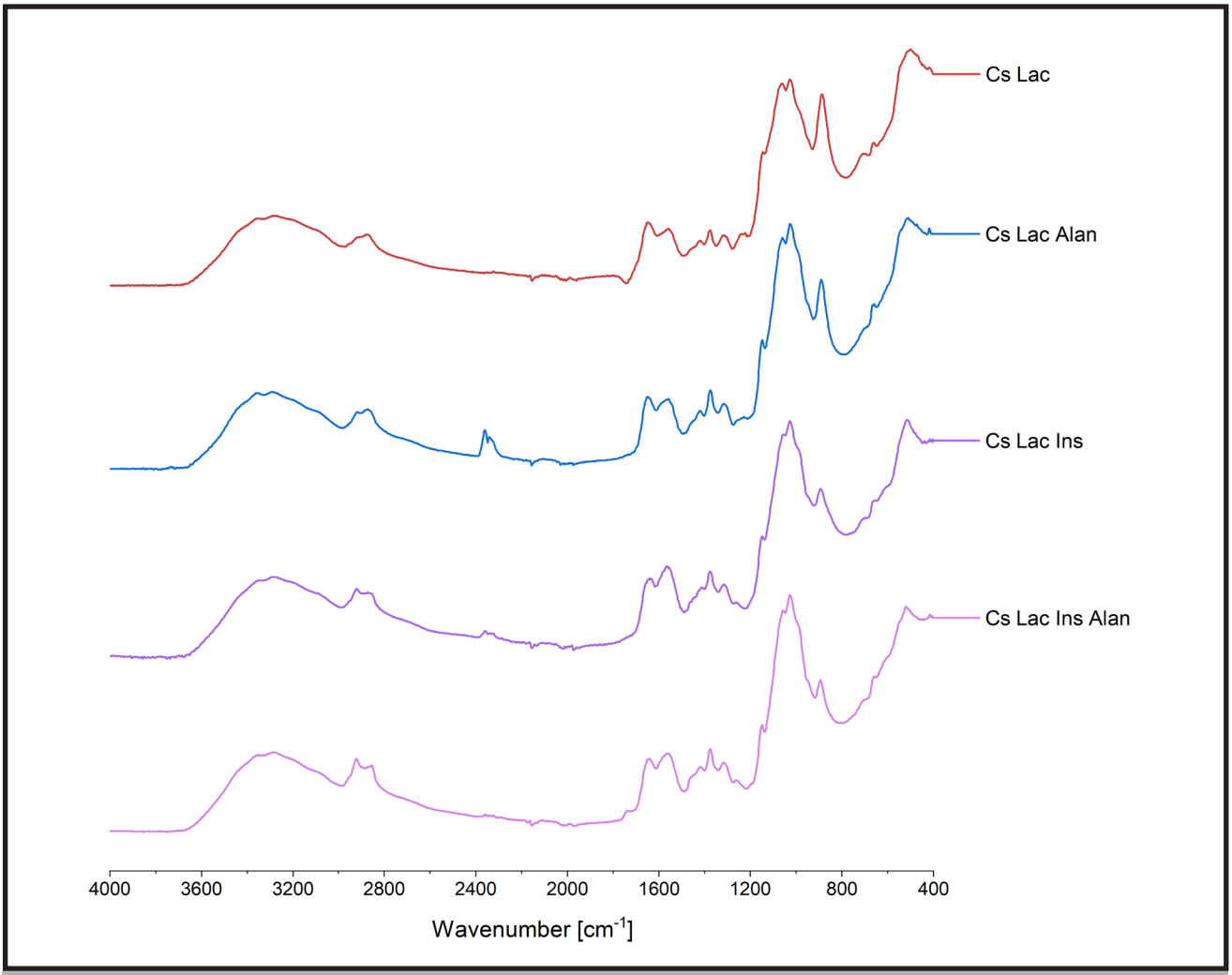

FIG. 8. FTIR spectra of lactic acid-based samples: Cs+Lac, Cs+Lac+Alan, Cs+Lac+Ins, and Cs+Lac+Ins+Alan.

TABLE 2. Summary of the main absorbance band shifts observed in lactic acid–based samples and their corresponding interpretations.

Cs Lac	Cs Lac Alan	Cs Lac Ins	Cs Lac Ins Alan	Vibration
2875 cm^{-1}	2873 cm^{-1}	2855 cm^{-1} 2817 cm^{-1}	2821 cm^{-1} 2817 cm^{-1}	N-H stretching in an amino group
1650 cm^{-1}	1648 cm^{-1}	1642 cm^{-1}	1643 cm^{-1}	C=N stretching in an imine group
1558 cm^{-1}	1558 cm^{-1}	1564 cm^{-1}	1563 cm^{-1}	N-H bending in an amino group
1060 cm^{-1}	1058 cm^{-1}	1054 cm^{-1}	1056 cm^{-1}	N-H bending in an amino group

and an increase in absorbance between 1055–990 cm^{-1} was noted in insulin-loaded samples.

As shown in FIG. 9, EDS analysis of the microsphere surface revealed nitrogen and sulfur contents of 9.31% and 1.55%, respectively. The elevated nitrogen level is attributed to the presence of both allantoin and insulin, while the detection of sulfur confirms insulin incorporation, owing to its characteristic disulfide bridges.

FTIR analysis confirmed the successful incorporation of allantoin and insulin into the chitosan microspheres. The observed shifts and intensity changes in the N–H stretching and bending regions, together with alterations in the amide I and II bands, indicate the formation of hydrogen bonds and intermolecular interactions among chitosan, allantoin, and insulin. These findings are consistent with previous reports on comparable systems, supporting the effective loading of the bioactive agents. EDS analysis further corroborated the FTIR results by revealing substantial nitrogen and sulfur content on the microsphere surfaces. Notably, the presence of sulfur serves as a direct marker of insulin incorporation, as sulfur is absent in chitosan and allantoin alone. This complementary evidence from FTIR and EDS provides strong confirmation of the microspheres' chemical composition and successful functionalization. Collectively, these results demonstrate that the fabrication process enables efficient encapsulation of both allantoin and insulin, which is essential for the intended therapeutic performance of the hydrogel dressing in diabetic wound healing.

Rheological properties tests

The mechanical strength, viscoelastic behavior, and cross-linking efficiency of the Alg-PVA hydrogels, both with and without allantoin, using varying concentrations of $ZnSO_4$ as the cross-linking agent, were tested. A summary of the results in the form of graphs is presented in FIGs 10–12.

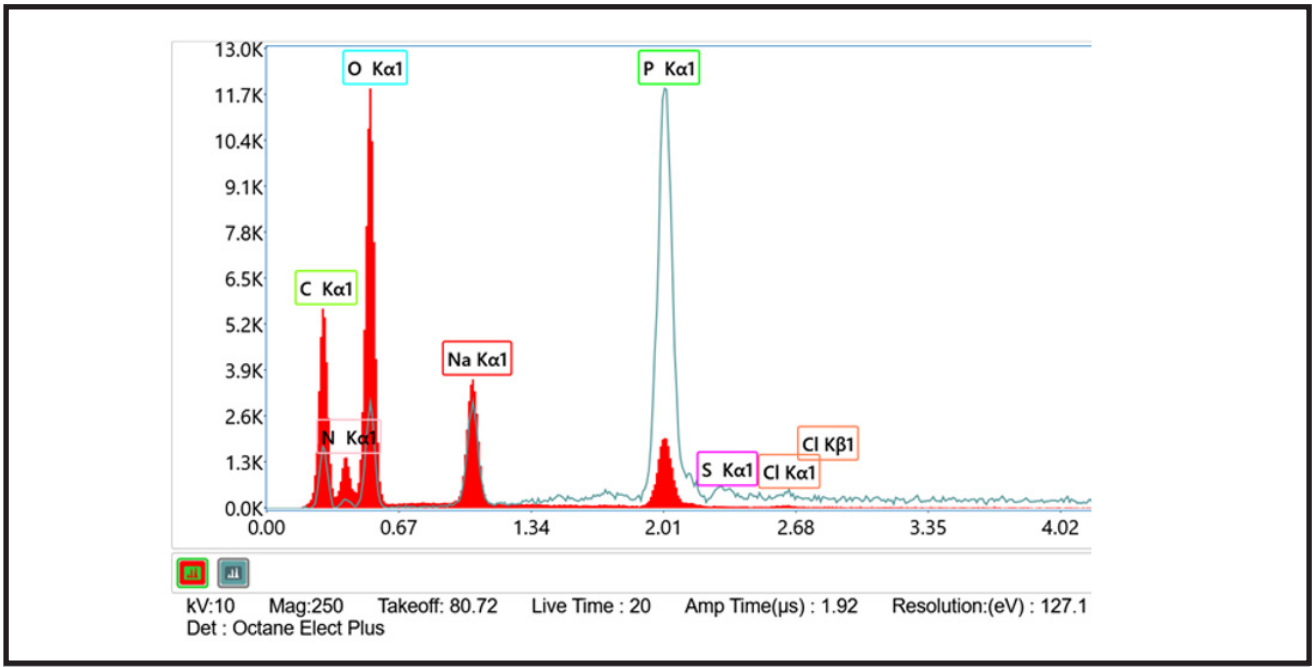

FIG. 9. Energy-dispersive X-ray spectroscopy (EDS) analysis of the microsphere surface.

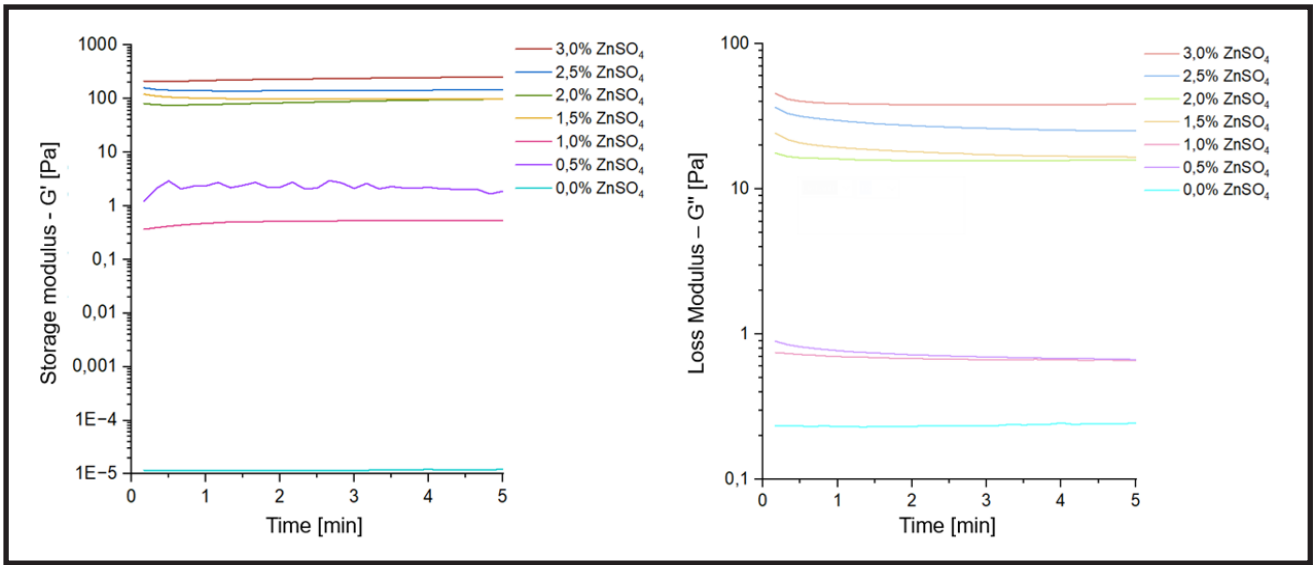

FIG. 10. Time-dependent storage modulus (G′, left) and loss modulus (G″, right) of Alg–PVA solution samples cross-linked with $ZnSO_4$ solutions at concentrations ranging from 0.5% to 3.0%.

The storage modulus (G') and loss modulus (G") were measured over time for Alg-PVA hydrogels cross-linked with $ZnSO_4$ concentrations ranging from 0.5% to 3.0%. At $ZnSO_4$ concentrations ≤1.0%, G" remained higher than G', indicating incomplete gelation and a predominantly viscous response. At 1.5% $ZnSO_4$, G' surpassed G", signifying the formation of a stable, cross-linked hydrogel network. Higher concentrations (≥2.0%) led to phase separation and heterogeneous cross-linking between the alginate and PVA phases. These findings align with previous studies [25, 26] that identify the G'/G" crossover point as a critical indicator of sol-gel transition in hydrogel systems. The results suggest that 1.5% $ZnSO_4$ is optimal for forming a mechanically stable Alg-PVA hydrogel without compromising homogeneity.

The hydrogel's mechanical strength under deformation was evaluated using shear stress-strain tests for samples cross-linked with 1.0% and 1.5% $ZnSO_4$, both with and without allantoin. All samples exhibited non-linear viscoelastic behavior, characteristic of weakly cross-linked hydrogels. The 1.5% $ZnSO_4$ cross-linked hydrogel had the highest shear resistance, confirming stronger gel formation. Samples containing allantoin demonstrated lower shear stress resistance,

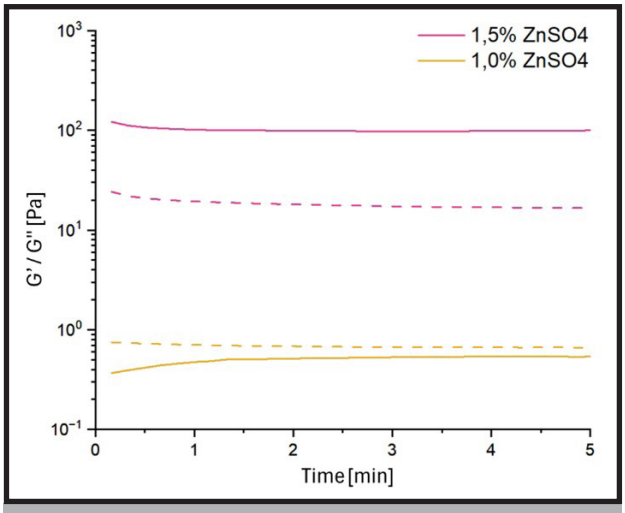

FIG. 11. Time-dependent storage (G′, solid line) and loss (G″, dashed line) moduli of Alg–PVA samples cross-linked with 1.0% and 1.5% $ZnSO_4$ solutions.

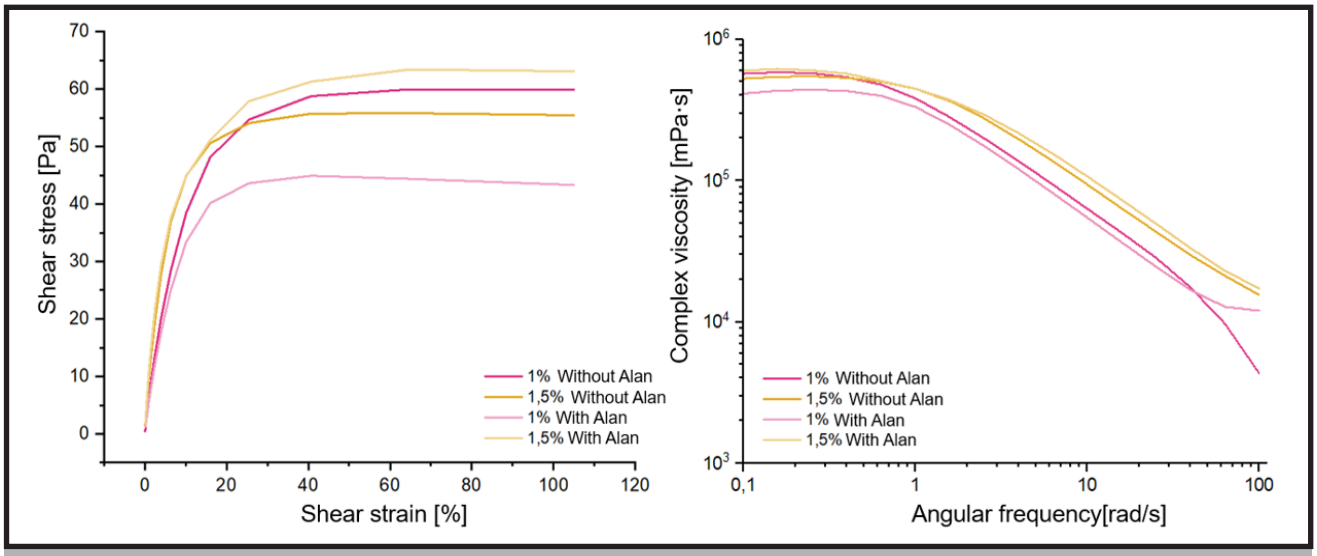

FIG. 12. (Left) Comparison of shear stress–strain curves for Alg–PVA samples cross-linked with 1.0% and 1.5% $ZnSO_4$ solutions, with allantoin (lighter colors) and without allantoin (darker colors). (Right) Storage (G′) and loss (G″) moduli as a function of angular frequency for Alg–PVA samples cross-linked with 1.0% and 1.5% $ZnSO_4$ solutions, containing allantoin (lighter colors) and without allantoin (darker colors).

suggesting that allantoin incorporation slightly weakened the hydrogel network's mechanical integrity. Comparing these results to prior work on PVA-alginate hydrogels [27], the mechanical properties are in line with soft, biocompatible hydrogels suitable for tissue engineering applications. However, further modifications might be required to enhance mechanical robustness for prolonged *in vivo* applications.

All samples exhibited typical gel-like behavior (G' > G") across the frequency range. The storage modulus remained nearly constant, indicating that the hydrogels maintained their elastic structure under varying stress conditions. No significant differences were observed between allantoin-modified and unmodified hydrogels, except for a slight decrease in G' in allantoin-containing samples, further supporting a mild reduction in cross-linking density. These trends correlate well with prior rheological studies on bioengineered hydrogels [28], suggesting that the developed Alg-PVA system maintains viscoelastic properties suitable for biomedical applications.

Chemical stability study

The results of the degradation study are summarized in TABLE 3. Hydrogel matrices from the Alg–PVA system, cross-linked with 1% and 1.5% $ZnSO_4$ solution, were evaluated using Ringer's solution. Based on mass measurements taken before and after exposure to Ringer's solution, the degree of matrix degradation was determined. Degradation was expressed as the percentage mass loss relative to the original mass of the matrix.

All hydrogel formulations demonstrated progressive mass loss throughout the 28-day incubation period. The majority of samples exhibited approximately 40% mass loss at day 28, indicative of moderate degradability suitable for biomedical applications. Notably, the small-volume hydrogel cross-linked with 1.5% $ZnSO_4$ displayed a lower mass loss (~25%), suggesting enhanced network density and structural stability. Degradation kinetics varied among samples. Most hydrogels underwent the most rapid degradation within the initial 7 days, followed by a slower,

TABLE 3. Masses of non-degraded samples (day 0) and degraded samples (days 7, 14, 21, and 28) following incubation in Ringer's solution.

Sample	Mass of the sample m [g]					Total degradation rate D [%]
	Day 0	Day 7	Day 14	Day 21	Day 28	
Small 1.0% $ZnSO_4$	1.53(5)	1.35(3)	1.12(9)	1.00(6)	0.92(3)	39.87 ± 0.050
Small 1.5% $ZnSO_4$	1.56(7)	1.35(3)	1.29(1)	1.22(6)	1.17(1)	25.271 ± 0.027
Large 1.0% $ZnSO_4$	2.85(7)	2.25(9)	1.98(7)	1.86(1)	1.61(2)	43.577 ± 0.031
Large 1.5% $ZnSO_4$	3.47(7)	2.45(7)	2.31(7)	2.10(5)	1.94(0)	44.205 ± 0.026

near-linear rate of mass loss thereafter. In contrast, the small-volume, 1.5% $ZnSO_4$-cross-linked hydrogel exhibited a consistent, linear degradation profile over the entire period, likely attributable to its compact morphology. When compared to methacrylated Alg-PVA hydrogels cross-linked via UV irradiation [23], the present formulations demonstrated comparable initial degradation but a higher cumulative mass loss after 28 days (over 40% versus 30%). This discrepancy may be attributed to differences in cross-linking chemistry and hydrogel composition. These findings indicate that Alg-PVA hydrogels cross-linked with $ZnSO_4$ possess tunable degradation rates, with higher cross-linker concentrations conferring greater resistance to hydrolytic breakdown. The observed degradation profiles suggest that these hydrogels maintain sufficient structural integrity for potential wound dressing applications, while allowing for gradual resorption *in vivo*.

Conclusions

The management of diabetic wounds is complicated by persistent inflammation, impaired angiogenesis, oxidative stress, and recurrent infections, all of which are enhanced by elevated blood glucose and the accumulation of advanced glycation end-products. In this study, we developed a multifunctional hydrogel dressing composed of a sodium alginate and poly(vinyl alcohol) matrix incorporating chitosan microspheres loaded with insulin and allantoin. This system was designed to address both the metabolic and regenerative challenges of diabetic wound healing by combining local glucose regulation with growth factor support.

The hydrogel dressing demonstrated high water absorption capacity, particularly in buffered, insulin-loaded microspheres, and enabled controlled release of insulin at the wound site. FTIR and EDS analyses confirmed the successful incorporation of both insulin and allantoin into the microsphere and hydrogel structures. The material exhibited moderate mechanical stability, with a mass loss of approximately 40% over 28 days, indicating a balance between durability and biodegradability suitable for wound healing applications.

Overall, the developed formulation shows strong potential as an advanced dressing for diabetic ulcers. Nevertheless, further optimization is required to improve its mechanical performance and microstructural organization. Future work will include a comprehensive *in vitro* biological evaluation to assess cytocompatibility, pro-regenerative activity, and therapeutic efficacy.

Acknowledgments

This study was supported by the subsidy (No 16.16.160.557) for the AGH University of Krakow.

References

[1] Cole J. B., Florez J. C.: Genetics of diabetes mellitus and diabetes complications. Nature reviews: Nephrology 16(7) (2020) 377–390.
[2] Armstrong D. G., Boulton A. J. M., Bus S. A.: Diabetic Foot Ulcers and Their Recurrence. The New England journal of medicine 376(24) (2017) 2367–2375.
[3] Matijević T., Talapko J., Meštrović T., Matijević M., Erić S., Erić I., Škrlec I.: Understanding the multifaceted etiopathogenesis of foot complications in individuals with diabetes. World journal of clinical cases 11(8) (2023) 1669–1683.
[4] Sorber R., Abularrage C. J.: Diabetic foot ulcers: Epidemiology and the role of multidisciplinary care teams. Seminars in vascular surgery 34(1) (2021) 47–53.
[5] Ramirez-Acuña J. M., Cardenas-Cadena S. A., Marquez-Salas P. A., Garza-Veloz I., Perez-Favila A., Cid-Baez M. A., Flores-Morales V., Martinez-Fierro, M. L.: Diabetic Foot Ulcers: Current Advances in Antimicrobial Therapies and Emerging Treatments. Antibiotics 8(4) (2019) 193.
[6] Xu Z., Han S., Gu Z.., Wu J. Advances and Impact of Antioxidant Hydrogel in Chronic Wound Healing. Advanced healthcare materials 9(5) (2020) 1901502
[7] Dasari N., Jiang A., Skochdopole A., Chung J., Reece E. M., Vorstenbosch J., Winocour S. Updates in Diabetic Wound Healing, Inflammation, and Scarring. Seminars in plastic surgery 35(3) (2021) 153–158.
[8] Deng L., Du C., Song P., Chen T., Rui S., Armstrong D. G., Deng W. The Role of Oxidative Stress and Antioxidants in Diabetic Wound Healing. Oxidative medicine and cellular longevity 2021 (2021) 8852759.
[9] Dai J., Chen H., Chai Y. Advanced Glycation End Products (AGEs) Induce Apoptosis of Fibroblasts by Activation of NLRP3 Inflammasome via Reactive Oxygen Species (ROS) Signaling Pathway. Medical science monitor: international medical journal of experimental and clinical research 25 (2019) 7499–7508.

[10] Wilkinson H. N., Hardman, M. J. Wound senescence: A functional link between diabetes and ageing?. Experimental dermatology 30(1) (2021) 68–73.
[11] Yang S., Gu Z., Lu C., Zhang T., Guo X., Xue G., Zhang L. Neutrophil Extracellular Traps Are Markers of Wound Healing Impairment in Patients with Diabetic Foot Ulcers Treated in a Multidisciplinary Setting. Advances in wound care 9(1) (2020), 16–27.
[12] Burgess J. L., Wyant W. A., Abdo Abujamra B., Kirsner R. S., Jozic, I. Diabetic Wound-Healing Science. Medicina 57(10) (2021) 1072.
[13] Kus K. J. B., Ruiz E. S.: Wound Dressings – A Practical Review. Current Dermatology Reports 9 (2020) 298-308.
[14] Brumberg V., Astrelina T., Malivanova T., Samoilov A.: Modern Wound Dressings: Hydrogel Dressings. Biomedicines 9 (2021) 1235.
[15] Firlar I., Altunbek M., McCarthy C., Ramalingam M., Camci-Unal G. Functional Hydrogels for Treatment of Chronic Wounds. Gels 8(2) (2022) 127.
[16] Huang C., Dong L., Zhao B., Lu Y., Huang S., Yuan Z., Luo G., Xu Y., Qian W.: Anti-inflammatory hydrogel dressings and skin wound healing. Clinical and Translational Medicine 12 (2022) 11.
[17] Shukla S. K., Sharma A. K., Gupta V., Yashavarddhan M. H.: Pharmacological control of inflammation in wound healing. Journal of tissue viability 28(4) (2019) 218–222.
[18] Ng L. C., Gupta M.: Transdermal drug delivery systems in diabetes management: A review. Asian journal of pharmaceutical sciences 15(1) (2020) 13–25.
[19] Sung Y.K., Kim S.W. Recent advances in polymeric drug delivery systems. Biomaterials Research 24 (2020) 12.
[20] Pachuau L. Recent developments in novel drug delivery systems for wound healing. Expert opinion on drug delivery 12(12) (2015) 1895–1909.
[21] Kłapcia A., Domalik-Pyzik P.: Hydrogel Dressings as Insulin Delivery Systems for Diabetic Wounds. Frontiers in Bioscience - Elite 17(1) (2025) 26446.
[22] Abouzeid R. E., Salama A., El-Fakharany E. M., Guarino V.: Preparation And Properties Of Novel Biocompatible Pectin/Silica Calcium Phosphate Hybrids. Cellulose Chemistry And Technology 56 (2022) 371-378.
[23] Manigandan A., Amruthavarshini P. R., Sethuraman S., Subramanian A.: Self-Standing Photo-Crosslinked Hydrogel Construct: in vitro Microphysiological Vascular Model. Cells Tissues Organs 211(3) (2022) 335–347.